Superelement reduction of substructures for sequential load calculations in OpenFAST

E. Branlard, M. Shields, B. Anderson, R. Damiani, F. Wendt, J. Jonkman, W. Musial

National Renewable Energy Laboratory, Golden, CO, USA

E-mail: emmanuel.branlard@nrel.gov

B. Foley

Keystone Engineering Inc., Metairie, LA, USA

Abstract. This article presents the superelement formulation newly implemented in *OpenFAST* to simulate fixed-bottom substructures with a reduced-order model similar to a common industry practice. The Guyan and Craig-Bampton methods are used to reduce the number of degrees of freedom and generate a so-called "superelement". The formulation allows manufacturers to exchange such superelements to perform load calculations without revealing sensitive information about the support structure (e.g., foundation, substructure, and/or tower) or turbine. The source code is made publicly available in the *OpenFAST* repository. Test cases with varying degrees of complexity are presented to validate the technique, and accuracy issues are discussed.

Abbreviations

CB	Craig Bampton
FEM	finite element method
DOF	degrees-of-freedom

1. Introduction

It is common practice in the offshore wind industry to perform sequentially coupled load analyses for fixed-bottom wind turbines [1, 2]. The process is illustrated in Figure 1. The substructure[1] designer performs a dynamic reduction of the structure. The reduction method used is typically the linear Craig-Bampton (CB) method [4], of which the Guyan [5] method is a special case. The outputs of the reduction are mass, damping, and stiffness matrices together with reduced forces (hydrodynamic and gravitational) at the interface with the tower. The wind turbine designers can then analyze aeroelastic loads on the tower and rotor nacelle assembly through an aero-servo-elastic code capable of simultaneously processing the CB information at the tower base and

[1] The International Electrotechnical Commission offshore standards [3] use the word *foundation* for the part of the structure below the mudline, and *substructure* for the part between the foundation and the tower. The superelement formulation presented in this document is applied to the substructure and foundation, but the term substructure will be used for conciseness. A different meaning to the term *substructure* will briefly be assigned in the context of dynamic system reduction.

Content from this work may be used under the terms of the Creative Commons Attribution 3.0 licence. Any further distribution of this work must maintain attribution to the author(s) and the title of the work, journal citation and DOI.
Published under licence by IOP Publishing Ltd

through the rest of the structure. The loads from the full turbine simulation are subsequently passed back to the substructure manufacturer to compute individual member loads. This is referred to as a sequential approach because the substructure and turbine designers perform time simulations separately and exchange interface loads and displacements iteratively.

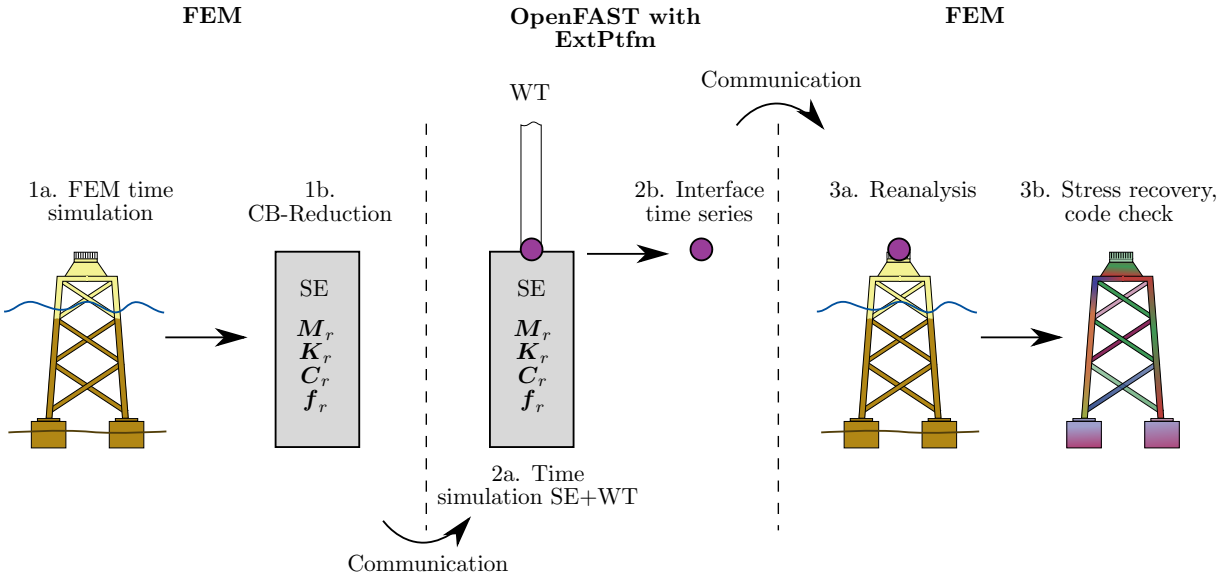

Figure 1: Simulation and communication steps in the sequential approach. The substructure designer typically uses a finite element method (FEM) software to generate a superelement (SE) using the Craig-Bampton (CB) reduction method. This SE is then used in an aeroelastic tool for a full substructure and wind turbine simulation. The interface time series from this tool is communicated back for reanalysis, stress recovery, and code check.

The superelement reduction technique allows for the respective intellectual properties of the turbine and substructure to be compartmentalized, while still accounting for all the interactions between the systems. The CB technique also improves the computational efficiency of the wind turbine system dynamic simulations by reducing the large number of degrees of freedom ($\approx 10^4$) associated with a standard finite-element analysis of a typical multimember structure. In theory, the level of fidelity in the overall system response can be maintained by guaranteeing that the substructure-reduced degrees-of-freedom (DOF) model retains the fundamental low-frequency response modes of the original finite-element model. Yet, the model is linear, and application of the sequential technique requires expertise, which has raised concerns on its accuracy [6, 7]. Previous work has presented the implementation of such methods into some of the aero-hydro-elastic codes used by the wind energy community, including *Flex* [8, 9], *HAWC2* [10], and *Bladed* [2]. This paper documents the implementation within the modular framework of *OpenFAST* [11].

The first part of this article briefly outlines the CB reduction technique and its representation in a state-space form, followed by a discussion of the *OpenFAST* implementation. The second part of the article presents test cases using analytical models and the Offshore Code Comparison Collaboration Continuation (OC4) jacket design. Results from *OpenFAST* and the commercial finite element method (FEM) package SACS [12] are provided. The final section of the article presents a discussion of the accuracy of the method and some general guidelines concerning its applicability.

2. Craig-Bampton reduction

2.1. Introduction

The CB reduction technique is briefly presented in this section; refer to the original paper describing the method for additional details [4]. The CB method is a technique that reduces the number of DOF of a system while trying to maintain sufficient accuracy to correctly represent the overall dynamics. The process of reducing the number of DOF is often referred to as condensation in the context of static analyses, whereas the term reduction is preferred for dynamic analyses. Static condensation is exact, whereas reduction techniques introduce approximations. In both approaches, the DOF are partitioned, and only a subset are retained. The equations are solved for the retained DOF, and the displacements, motions, and loads at the eliminated DOF can be retrieved as a postprocessing step called recovery. The choice of retained DOF may be dictated by the boundary conditions or may be arbitrary, but in general, different choices will lead to various levels of accuracy. When a system is made of different macrostructures, these structures may be reduced, and the retained DOF are usually chosen as boundary DOF that interact with the other macroelements; while the other DOF are referred to as internal DOF. A reduced macroelement is then referred to as a superelement, and the process of dividing a structure into macroelements is called substructuring. In the context of this analysis, the turbine, tower, and substructure are the macroelements under consideration.

In many cases found in FEM analyses, the terms retained, boundary, and master DOF are synonyms, with their counterparts being eliminated, internal, and slave DOF, respectively. The terms leader and follower will be used in this document instead of master and slave. In the CB technique, the system is first partitioned into a set of leader and follower DOF; then an eigenvalue analysis is performed on the constrained follower DOF, and a subset of the modes are selected. The retained DOF are the set of the leader DOF, and the selected follower modal DOF; the latter of these represent the internal modes of the system.

2.2. Reduction of the equations of motion

The dynamics of a structure are defined by $\boldsymbol{M}\ddot{\boldsymbol{x}}+\boldsymbol{C}\dot{\boldsymbol{x}}+\boldsymbol{K}\boldsymbol{x}=\boldsymbol{f}$, where $\boldsymbol{M}$, $\boldsymbol{C}$, $\boldsymbol{K}$ are the mass, damping, and stiffness matrices; $\boldsymbol{x}$ is the vector of DOF; and $\boldsymbol{f}$ is the vector of loads acting on the DOF. In the current application, this system of equations is set up for the support structure, either by a commercial software or by the *SubDyn* module of *OpenFAST*. The typical number of DOF for a jacket substructure is about 10^3 to 10^4. The DOF are first partitioned and rearranged into a set of leader and follower DOF, labelled with the subscript l and f, respectively. In the case of the substructure, the six degrees of freedom corresponding to the three translations and rotations of the interface point between the substructure and the tower are selected as leader DOF. Assuming symmetry of the system matrices, the rearranged equation of motions are:

$$\begin{bmatrix} \boldsymbol{M}_{\ell\ell} & \boldsymbol{M}_{\ell f} \\ \boldsymbol{M}_{\ell f}^t & \boldsymbol{M}_{ff} \end{bmatrix} \begin{bmatrix} \ddot{\boldsymbol{x}}_\ell \\ \ddot{\boldsymbol{x}}_f \end{bmatrix} + \begin{bmatrix} \boldsymbol{C}_{\ell\ell} & \boldsymbol{C}_{\ell f} \\ \boldsymbol{C}_{\ell f}^t & \boldsymbol{C}_{ff} \end{bmatrix} \begin{bmatrix} \dot{\boldsymbol{x}}_\ell \\ \dot{\boldsymbol{x}}_f \end{bmatrix} + \begin{bmatrix} \boldsymbol{K}_{\ell\ell} & \boldsymbol{K}_{\ell f} \\ \boldsymbol{K}_{\ell f}^t & \boldsymbol{K}_{ff} \end{bmatrix} \begin{bmatrix} \boldsymbol{x}_\ell \\ \boldsymbol{x}_f \end{bmatrix} = \begin{bmatrix} \boldsymbol{f}_\ell \\ \boldsymbol{f}_f \end{bmatrix} \tag{1}$$

The CB reduction assumes that the followers' motion consists of two parts: (1) the elastic motion that would occur in response to the motion of the leader DOF if the inertia of the followers and the external forces were neglected; and (2) the internal motion that would result from the external forces directly exciting the internal DOF. The first part is effectively obtained from Equation 1 by assuming statics[2] and solving for $\boldsymbol{x}_f$, leading to:

$$\boldsymbol{x}_{f,\text{Guyan}} = -\boldsymbol{K}_{ff}^{-1}\boldsymbol{K}_{\ell f}^t\,\boldsymbol{x}_{\ell,\text{Guyan}} = \boldsymbol{\Phi}_1\boldsymbol{x}_{\ell,\text{Guyan}}, \quad \text{where} \quad \boldsymbol{\Phi}_1 \triangleq -\boldsymbol{K}_{ff}^{-1}\boldsymbol{K}_{\ell f}^t \tag{2}$$

[2] Equivalently, the result is obtained by setting the inertia terms $(\boldsymbol{M}_{\ell f}, \boldsymbol{M}_{ff})$, the external forces $(\boldsymbol{f}_f)$, and the damping terms to $\boldsymbol{0}$.

Equation 2 provides the motion of the followers as a function of the leaders' motion under the assumptions of the Guyan reduction [5].

The CB method further considers the isolated and undamped eigenvalue problem of the follower DOF: $\left(\boldsymbol{K}_{ff} - \nu_i^2 \boldsymbol{M}_{\text{ff}}\right) \boldsymbol{\phi}_i = 0$ where ν_i and $\boldsymbol{\phi}_i$ are the i^{th} angular frequency and mode shape, respectively; this problem is "constrained" because it inherently assumes that the leader DOF are fixed (i.e., zero). The method next selects n_{CB} mode shapes, gathering them as column vectors into a matrix noted $\boldsymbol{\Phi}_2$. These mode shapes can be selected as the ones with the lowest frequency or a mix of low- and high-frequency mode shapes. Typically, n_{CB} is several orders of magnitude smaller than the original number of DOF, going from $\sim 10^3$ DOF to ~ 20 modes for a wind turbine substructure. The scaling of the modes is chosen such that $\boldsymbol{\Phi}_2^t \boldsymbol{M}_{ff} \boldsymbol{\Phi}_2 = \boldsymbol{I}$, where $\boldsymbol{I}$ is the identity matrix. Effectively, the CB method performs a change of coordinates from the full set, $\boldsymbol{x} = [\boldsymbol{x}_l \ \boldsymbol{x}_f]^t$, to the reduced set, $\boldsymbol{x}_r = [\boldsymbol{x}_{r1} \ \boldsymbol{x}_{r2}]^t$, where $\boldsymbol{x}_{r1}$ corresponds directly to the leader DOF, whereas $\boldsymbol{x}_{r2}$ are the modal coordinates defining the amplitudes of each of the mode shapes selected. The change of variable is formally written as:

$$\begin{bmatrix} \boldsymbol{x}_l \\ \boldsymbol{x}_f \end{bmatrix} \approx \begin{bmatrix} \boldsymbol{I} & \boldsymbol{0} \\ \boldsymbol{\Phi}_1 & \boldsymbol{\Phi}_2 \end{bmatrix} \begin{bmatrix} \boldsymbol{x}_{r1} \\ \boldsymbol{x}_{r2} \end{bmatrix} \quad \Leftrightarrow \quad \boldsymbol{x} \approx \boldsymbol{T}\boldsymbol{x}_r, \quad \text{with} \quad \boldsymbol{T} \triangleq \begin{bmatrix} \boldsymbol{I} & \boldsymbol{0} \\ \boldsymbol{\Phi}_1 & \boldsymbol{\Phi}_2 \end{bmatrix} \tag{3}$$

The equations of motion are rewritten in these coordinates by the transformation: $\boldsymbol{M}_r \triangleq \boldsymbol{T}^t \boldsymbol{M} \boldsymbol{T}$, $\boldsymbol{K}_r \triangleq \boldsymbol{T}^t \boldsymbol{K} \boldsymbol{T}$, $\boldsymbol{f}_r \triangleq \boldsymbol{T}^t \boldsymbol{f}$, leading to $\boldsymbol{M}_r \ddot{\boldsymbol{x}}_r + \boldsymbol{K}_r \boldsymbol{x}_r = \boldsymbol{f}_r$, which is written in a developed form as:

$$\begin{bmatrix} \boldsymbol{M}_{r11} & \boldsymbol{M}_{r12} \\ \boldsymbol{M}_{r12}^t & \boldsymbol{M}_{r22} \end{bmatrix} \begin{bmatrix} \ddot{\boldsymbol{x}}_{r1} \\ \ddot{\boldsymbol{x}}_{r2} \end{bmatrix} + \begin{bmatrix} \boldsymbol{K}_{r11} & \boldsymbol{0} \\ \boldsymbol{0} & \boldsymbol{K}_{r22} \end{bmatrix} \begin{bmatrix} \boldsymbol{x}_{r1} \\ \boldsymbol{x}_{r2} \end{bmatrix} = \begin{bmatrix} \boldsymbol{f}_{r1} \\ \boldsymbol{f}_{r2} \end{bmatrix} \tag{4}$$

with

$$\begin{aligned} &\boldsymbol{M}_{r11} = \boldsymbol{M}_{\ell\ell} + \boldsymbol{\Phi}_1^t \boldsymbol{M}_{f\ell} + \boldsymbol{M}_{\ell f} \boldsymbol{\Phi}_1 + \boldsymbol{\Phi}_1^t \boldsymbol{M}_{ff} \boldsymbol{\Phi}_1, \qquad && \boldsymbol{M}_{r22} = \boldsymbol{\Phi}_2^t \boldsymbol{M}_{ff} \boldsymbol{\Phi}_2 = \boldsymbol{I} \\ &\boldsymbol{M}_{r12} = \left(\boldsymbol{M}_{\ell f} + \boldsymbol{\Phi}_1^t \boldsymbol{M}_{ff}\right) \boldsymbol{\Phi}_2, \qquad && \boldsymbol{f}_{r2} = \boldsymbol{\Phi}_2^t \boldsymbol{f}_f, \qquad \boldsymbol{f}_{r1} = \boldsymbol{f}_\ell + \boldsymbol{\Phi}_1^t \boldsymbol{f}_f \\ &\boldsymbol{K}_{r11} = \boldsymbol{K}_{\ell\ell} + \boldsymbol{K}_{\ell f} \boldsymbol{\Phi}_1, \qquad && \boldsymbol{K}_{r22} = \boldsymbol{\Phi}_2^t \boldsymbol{K}_{ff} \boldsymbol{\Phi}_2 \end{aligned}$$

The expressions for the reduced damping matrix, $\boldsymbol{C}_r \triangleq \boldsymbol{T}^t \boldsymbol{C} \boldsymbol{T}$, are similar to the ones from the mass matrix, except that $\boldsymbol{C}_{r22}$ is not equal to the identity matrix. Some tools or practitioners may not compute the reduced damping matrix and instead set it based on the Rayleigh damping assumption, using the reduced mass and stiffness matrix. Setting $\boldsymbol{\Phi}_2 \equiv 0$ in Equation 4, or equivalently $n_{\text{CB}} \equiv 0$, leads to the Guyan reduction equations.

2.3. Coupling with another structure

This section illustrates how the equations of motions are set when a superelement is coupled to another structure. The superelement is here assumed to represent the substructure (and foundation), but it may be applied to other parts of the wind turbine, in particular the entire support structure (see footnote 1). For simplicity, it is assumed here that all the substructure leader DOF have an interface with the remaining part of the structure. The interface DOF are labelled as index 1, the substructure internal DOF as index 2, and the remaining DOF are labelled 0. The subscript r used in the previous paragraph is dropped for the DOF but kept for the matrices. With this labelling, system 0–1 consists of the tower and rotor nacelle assembly, the system 1–2 is the substructure, and the vector, $\boldsymbol{x}_1$, is the six degrees of freedom at the top of the transition piece. The damping terms are omitted to simplify the equations, but their inclusion is straightforward. Two ways to set up the equations of motions are presented next, the monolithic or modular approaches.

Monolithic approach In this approach, the full system of equations is solved with all the DOF gathered into one state vector. The system of equations is obtained by assembling the individual mass and stiffness matrices of the different subsystems. Using Equation 4, the equations of motion of the system written in a monolithic form are:

$$\begin{bmatrix} \boldsymbol{M}_{00} & \boldsymbol{M}_{01} & \boldsymbol{0} \\ & \boldsymbol{M}_{11}+\boldsymbol{M}_{r11} & \boldsymbol{M}_{r12} \\ \text{sym} & & \boldsymbol{M}_{r22} \end{bmatrix} \begin{bmatrix} \ddot{\boldsymbol{x}}_0 \\ \ddot{\boldsymbol{x}}_1 \\ \ddot{\boldsymbol{x}}_2 \end{bmatrix} + \begin{bmatrix} \boldsymbol{K}_{00} & \boldsymbol{K}_{01} & \boldsymbol{0} \\ & \boldsymbol{K}_{11}+\boldsymbol{K}_{r11} & \boldsymbol{0} \\ \text{sym} & & \boldsymbol{K}_{r22} \end{bmatrix} \begin{bmatrix} \boldsymbol{x}_0 \\ \boldsymbol{x}_1 \\ \boldsymbol{x}_2 \end{bmatrix} = \begin{bmatrix} \boldsymbol{f}_0 \\ \boldsymbol{f}_1+\boldsymbol{f}_{r1} \\ \boldsymbol{f}_{r2} \end{bmatrix} \quad (5)$$

Modular approach In this approach, the equations of motion are written for each subsystem. Couplings with other subsystems are introduced using external loads and constraints (which are unnecessary here). The coupling load vector at 1 between the two systems, usually consisting of three forces and three moments, is written as $\boldsymbol{f}_C$. The equations of motion for system 0–1 are:

$$\begin{bmatrix} \boldsymbol{M}_{00} & \boldsymbol{M}_{01} \\ \text{sym} & \boldsymbol{M}_{11} \end{bmatrix} \begin{bmatrix} \ddot{\boldsymbol{x}}_0 \\ \ddot{\boldsymbol{x}}_1 \end{bmatrix} + \begin{bmatrix} \boldsymbol{K}_{00} & \boldsymbol{K}_{01} \\ \text{sym} & \boldsymbol{K}_{11} \end{bmatrix} \begin{bmatrix} \boldsymbol{x}_0 \\ \boldsymbol{x}_1 \end{bmatrix} = \begin{bmatrix} \boldsymbol{f}_0 \\ \boldsymbol{f}_1 \end{bmatrix} + \begin{bmatrix} \boldsymbol{0} \\ \boldsymbol{f}_C \end{bmatrix} \quad (6)$$

System $1-2$ receives the opposite , $\boldsymbol{f}_C$, from system $0-1$, leading to the following set of equations for system 1–2:

$$\begin{bmatrix} \boldsymbol{M}_{r11} & \boldsymbol{M}_{r12} \\ \text{sym} & \boldsymbol{M}_{r22} \end{bmatrix} \begin{bmatrix} \ddot{\boldsymbol{x}}_1 \\ \ddot{\boldsymbol{x}}_2 \end{bmatrix} + \begin{bmatrix} \boldsymbol{K}_{r11} & \boldsymbol{0} \\ \text{sym} & \boldsymbol{K}_{r22} \end{bmatrix} \begin{bmatrix} \boldsymbol{x}_1 \\ \boldsymbol{x}_2 \end{bmatrix} = \begin{bmatrix} \boldsymbol{f}_{r1} \\ \boldsymbol{f}_{r2} \end{bmatrix} - \begin{bmatrix} \boldsymbol{f}_C \\ \boldsymbol{0} \end{bmatrix} \quad (7)$$

3. *OpenFAST* implementation for the support structure

3.1. Introduction

The aero-hydro-servo-elastic program *OpenFAST* [11] is a dedicated tool, written using a modular framework, and intended for wind turbine time domain simulations. The current modules available to model the support structure are *SubDyn* and *ExtPtfm*, while the hydrodynamic loads are computed by *HydroDyn*. The different modules and modeling options are illustrated in Figure 2. The previous implementation of *ExtPtfm* used a Guyan reduction approach to model the support structure. The following sections will detail the implementation of the CB approach into *ExtPtfm* to model fixed-bottom substructures. This new implementation of the module uses superelement properties (e.g., mass, stiffness, damping, and time series of excitation forces) that are provided by the user. These properties are not computed internally by the module.

SubDyn [13] models a substructure using a Timoshenko finite element beam formulation and has the option to perform a CB reduction. The main difference with the new implementation of *ExtPtfm* is that in *SubDyn* the hydrodynamics are computed with an external module and provided at each time step to *SubDyn*.

Full wind turbine simulations with a fixed-bottom substructure may be performed in three different ways in *OpenFAST* (see Figure 2): (1) using the module *ExtPtfm* (superelement approach), (2) using the module *SubDyn* without CB reduction (fully integrated), or (3) using the *SubDyn* module with CB reduction (fully integrated with reduction). These different approaches will be used to validate the *ExtPtfm* implementation and discuss the accuracy of the results.

3.2. Typical sequentially coupled workflow with ExtPtfm

The overall workflow includes the following steps:

- The substructure designer performs a time-domain simulation of the isolated substructure under a given sea state, using a high-fidelity tool such as a finite-element tool. The high-fidelity model and time series of loads are reduced using the CB technique described in

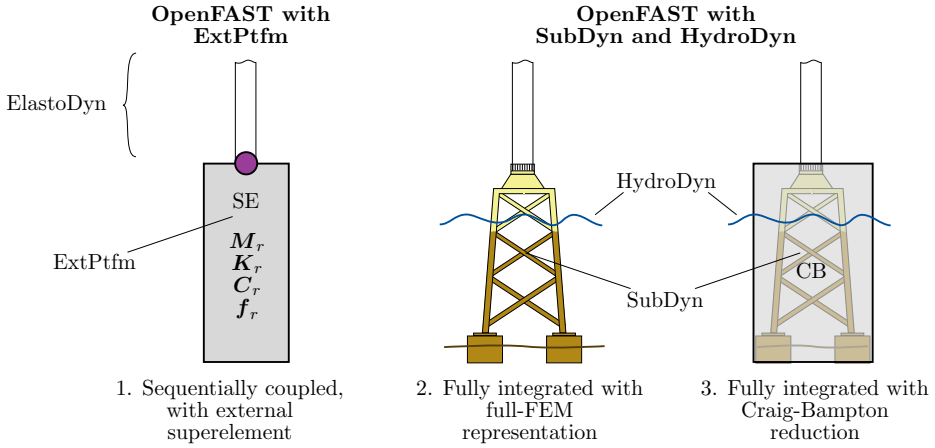

Figure 2: Sketch of the three different options to model a wind turbine with a substructure in *OpenFAST*

section 2, where the leader DOF are selected as the ones at the substructure interface node. Results from the reduction are written to a file containing the reduced system matrices, $\boldsymbol{M}_r$, $\boldsymbol{C}_r$, $\boldsymbol{K}_r$, and the time series of reduced loads, $\boldsymbol{f}_r$.

- The file is imported in *OpenFAST* by the *ExtPtfm* module, and a time-domain simulation of the full wind turbine is run with the reduced representation of the substructure. At every time step, the *ExtPtfm* module inputs the displacement, velocity, and acceleration of the interface point and returns the loads at this point.
- *OpenFAST* exports times series of loads and displacements at the interface, which are then returned to the substructure designer. These inputs are used as boundary conditions to the high-fidelity tool and then another time-domain simulation of the substructure is run. Stress concentrations are computed, and code checks are performed.

Details of the *OpenFAST* implementation are given in the following paragraphs.

3.3. State-space representation of the module ExtPtfm

ExtPtfm provides the coupling load at the interface, $\boldsymbol{f}_C$, given the motions of the interface node: $\boldsymbol{x}_1$, $\dot{\boldsymbol{x}}_1$, $\ddot{\boldsymbol{x}}_1$. The six degrees of freedom, $\boldsymbol{x}_1$—surge, sway, heave, roll, pitch, and yaw—and the coordinate system used at the interface are given in Figure 3. Following the modularization

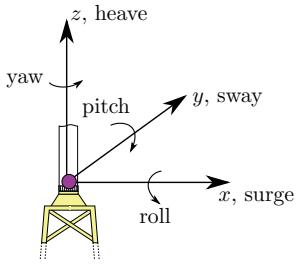

Figure 3: Coordinate systems at the interface point and the six degrees of freedom of this node

framework adopted in *OpenFAST* [14, 15], *ExtPtfm* is written in a form that consists of state and output equations. For a linear system, these equations take the following form:

$$\dot{\boldsymbol{x}} = \boldsymbol{X}(\boldsymbol{x}, \boldsymbol{u}, t) = \boldsymbol{A}\boldsymbol{x} + \boldsymbol{B}\boldsymbol{u} + \boldsymbol{f}_x, \qquad \boldsymbol{y} = \boldsymbol{Y}(\boldsymbol{x}, \boldsymbol{u}, t) = \boldsymbol{C}\boldsymbol{x} + \boldsymbol{D}\boldsymbol{u} + \boldsymbol{f}_y \tag{8}$$

where $\boldsymbol{x}$ is the state vector, $\boldsymbol{u}$ the input vector, and $\boldsymbol{y}$ the output vector of the module. The input vector of the module is the motion of the interface node, $\boldsymbol{u} = [\boldsymbol{x}_1, \dot{\boldsymbol{x}}_1, \ddot{\boldsymbol{x}}_1]^t$, whereas the

output vector is the coupling load at the interface node, $\boldsymbol{y} = [\boldsymbol{f}_C]^t$. The state vector consists of the motions and velocities of the CB modes, $\boldsymbol{x} = [\boldsymbol{x}_2, \dot{\boldsymbol{x}}_2]^t$. The dimensions of each vector are: $\boldsymbol{x}(2n_{\text{CB}} \times 1)$, $\boldsymbol{u}(18 \times 1)$, $\boldsymbol{y}(6 \times 1)$.

Equation 7 is rewritten in the state-space form of Equation 8 as follows. The second block row of Equation 7 is developed to isolate $\ddot{\boldsymbol{x}}_2$. Using $\boldsymbol{M}_{r22} = \boldsymbol{I}$ and reintroducing the damping matrix for completeness gives:

$$\ddot{\boldsymbol{x}}_2 = \boldsymbol{f}_{r2} - \boldsymbol{M}_{r12}^t \ddot{\boldsymbol{x}}_1 - \boldsymbol{K}_{r22}\boldsymbol{x}_2 - \boldsymbol{C}_{r12}^t \dot{\boldsymbol{x}}_1 - \boldsymbol{C}_{r22}\dot{\boldsymbol{x}}_2 \tag{9}$$

The matrices of the state-space relation from Equation 8 are then directly identified as:

$$\boldsymbol{A} = \begin{bmatrix} \boldsymbol{0} & \boldsymbol{I} \\ -\boldsymbol{K}_{r22} & -\boldsymbol{C}_{r22} \end{bmatrix}, \qquad \boldsymbol{B} = \begin{bmatrix} \boldsymbol{0} & \boldsymbol{0} & \boldsymbol{0} \\ \boldsymbol{0} & -\boldsymbol{C}_{r12}^t & -\boldsymbol{M}_{r12}^t \end{bmatrix}, \qquad \boldsymbol{f}_x = \begin{bmatrix} \boldsymbol{0} \\ \boldsymbol{f}_{r2} \end{bmatrix} \tag{10}$$

Isolating $\boldsymbol{f}_C$ from the first block row of Equation 7 and using the expression of $\ddot{\boldsymbol{x}}_2$ from Equation 9 leads to:

$$\begin{aligned} \boldsymbol{f}_C =& \boldsymbol{f}_{r1} - \boldsymbol{M}_{r11}\ddot{\boldsymbol{x}}_1 - \boldsymbol{C}_{r11}\dot{\boldsymbol{x}}_1 - \boldsymbol{C}_{r12}\dot{\boldsymbol{x}}_2 - \boldsymbol{K}_{r11}\boldsymbol{x}_1 \\ & - \boldsymbol{M}_{r12}(\boldsymbol{f}_{r2} - \boldsymbol{M}_{r12}^t \ddot{\boldsymbol{x}}_1 - \boldsymbol{C}_{r12}^t \dot{\boldsymbol{x}}_1 - \boldsymbol{C}_{r22}\dot{\boldsymbol{x}}_2 - \boldsymbol{K}_{r22}\boldsymbol{x}_2) \end{aligned} \tag{11}$$

The matrices of Equation 8 for the output $\boldsymbol{y}$ are then identified as:

$$\boldsymbol{C} = \begin{bmatrix} \boldsymbol{M}_{r12}\boldsymbol{K}_{r22} & \boldsymbol{M}_{r12}\boldsymbol{C}_{r22} - \boldsymbol{C}_{r12} \end{bmatrix}, \qquad \boldsymbol{f}_y = \begin{bmatrix} \boldsymbol{f}_{r1} - \boldsymbol{M}_{r12}\boldsymbol{f}_{r2} \end{bmatrix} \tag{12}$$

$$\boldsymbol{D} = \begin{bmatrix} -\boldsymbol{K}_{r11} & -\boldsymbol{C}_{r11} + \boldsymbol{M}_{r12}\boldsymbol{C}_{r12}^t & -\boldsymbol{M}_{r11} + \boldsymbol{M}_{r12}\boldsymbol{M}_{r12}^t \end{bmatrix} \tag{13}$$

All the block matrices and vectors labeled with "r" are provided to the module via an input file. At a given time step, the loads, $\boldsymbol{f}_r(t)$, are computed by linear interpolation of the loads given in the input file, and the state equation, Equation 8, is solved for $\boldsymbol{x}$ with the outputs returned to the glue code of *OpenFAST*.

The glue code can also perform the linearization of the full system at a given time or operating point, using the Jacobians of the state equations of each module. Since the formulation of *ExtPtfm* is linear, the Jacobian of the state and output equations, with respect to the states and inputs of the module, are:

$$\frac{\partial \boldsymbol{X}}{\partial \boldsymbol{x}} = \boldsymbol{A}, \quad \frac{\partial \boldsymbol{Y}}{\partial \boldsymbol{x}} = \boldsymbol{C}, \quad \frac{\partial \boldsymbol{X}}{\partial \boldsymbol{u}} = \boldsymbol{B}, \quad \frac{\partial \boldsymbol{Y}}{\partial \boldsymbol{u}} = \boldsymbol{D} \tag{14}$$

4. Validation cases

We conducted a series of validation cases for the new *ExtPtfm* module, in which the CB reduction was implemented within *OpenFAST*. Global displacements of the OC4-jacket substructure (see [16]) were compared with finite element simulations from the commercial industry software package, Offshore Structural Analysis and Design Software (SACS) and direct *OpenFAST* runs. A visualization of the jacket and a description of the SACS and *SubDyn* models are given in Figure 4. Damping was defined for the finite element simulations using a Rayleigh damping assumption ($\mathbf{C} = \alpha\mathbf{M} + \beta\mathbf{K}$) with $\alpha = 0.10671$ s^1 and $\beta = 0.00061$ s. These values were selected to give a damping ratio of 1% of critical damping for the first two reduced modes. The damping matrix of the superelement accounts for both the hydrodynamic and structural damping, and its elements are, in general, evaluated by the substructure designer. For the current study, Rayleigh damping parameters were agreed upon. The goal of the testing is to characterize how effectively the reduced-order model, which is the basis of the sequentially coupled methodology, captures the full system dynamics for test cases with increasing degrees of complexity. All the reduced results presented in this paper used 25 CB modes. The 25 lowest frequency modes were selected, yet future work could consider a combination of high- and low-frequency modes (see section 5). A convergence study on the number of modes will also be considered. The results are presented in the following sections.

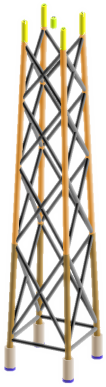

Figure 4: Visualization of the OC4 jacket. The jacket consists of 112 members. The SACS and SubDyn FEMs use Timoshenko beam elements with a total number of DOF on the order of 10^3. The wave loads are determined using Morison's formulation on individual members. Fixed boundary conditions were applied at the bottom of the structure (below the mudline). Each color on the figure represents a set of member properties (e.g., diameter, thickness, density, and moduli).

4.1. Analytical test cases

We ran simple test cases to validate the implementation. Results are not shown for conciseness, but the procedures are presented for potential inspiration. The time-integration scheme was validated using forced harmonic vibrations of the CB modes comprised of system matrices with no couplings between the interface and CB modes (i.e., the "1–2" matrices set to zero). Results were validated against the analytical solution for a single DOF system. Next, the free decay of a uniform beam in a vacuum with an initial deflection was used to validate the method. The frequency, damping, and response were then validated against FEM results and numerical results, using a superposition of mode shapes, as presented in [9]. Excellent agreement was found for these simple cases.

4.2. Jacket with applied point load and hydrodynamic damping

Following the successful comparisons with the simple beam element geometry, tests were conducted using the OC4 jacket substructure described in [16]. A point load, further referred to as a "push-drop" load, was applied to the jacket reference point in the x-direction and linearly increased from zero to a magnitude of 5×10^3 kN over 5 s before being released. The subsequent free decay of the structure was compared between the commercial finite element solver SACS and the *ExtPtfm* implementation in *OpenFAST*. No wave loads were applied, but the structure was surrounded by quiescent water to provide hydrodynamic damping. The push-drop case could not be simulated with *SubDyn*, but a similar free-decay test was run. The time and frequency domain results of the platform surge DOF are provided in Figure 5. Comparing the two FEM

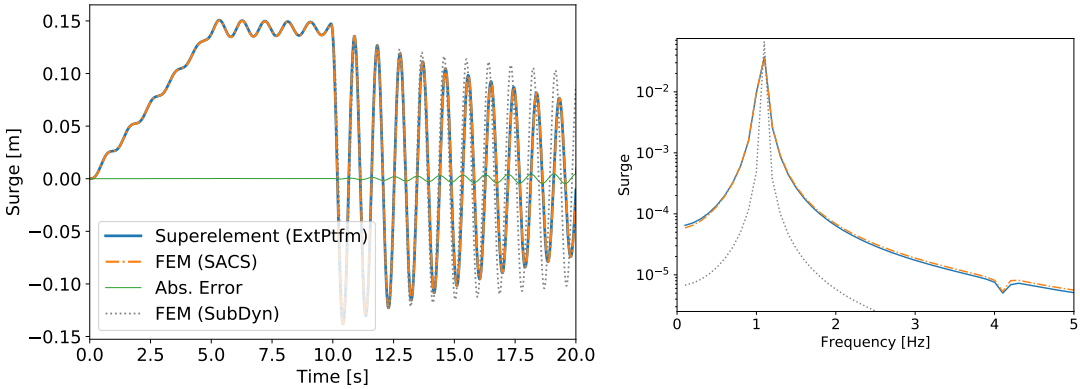

Figure 5: Jacket decay test in still water. Comparison of platform surge time series for finite element simulation and superelement representation of the OC4 jacket subjected to a "push-drop" load. (Left:) Time domain. (Right:) Power spectral density of surge, sway and heave displacements.

models, the *SubDyn* model appears to have lower damping, and a close inspection reveals that the first mode of the model is 2% higher than the one from SACS. Such difference explains the drift observed on Figure 5. We will keep this in mind to interpret the following results, and future studies may attempt to tune the *SubDyn* model to better match the SACS model. Comparison between the SACS FEM simulation and the reduced-order model representation (*ExtPtfm*) shows no observable differences in the time response or the frequency content. The mean relative error between the two simulations is below 1%. The superelement produced by the finite element solver is clearly able to capture the primary modal response of the structure. This result provides sufficient confidence to progress to a more complex load scenario.

4.3. Jacket under hydrodynamic loading

Wave loading was applied to the OC4 jacket substructure defined in [16]; this corresponds to the A001 design load case identified in a previous phase of this work (see [17]), which is a subset of (IEC) design standard 61400-3 [3], although wind loads were not applied. Similar to the previous test case, the loads were applied within the commercial finite element solver, and the subsequently reduced CB matrices and load time series were used by *OpenFAST* through the *ExtPtfm* module. The time and frequency domain results of the platform DOF are plotted in Figure 6. Again, the results of the superelement implementation closely match the finite element

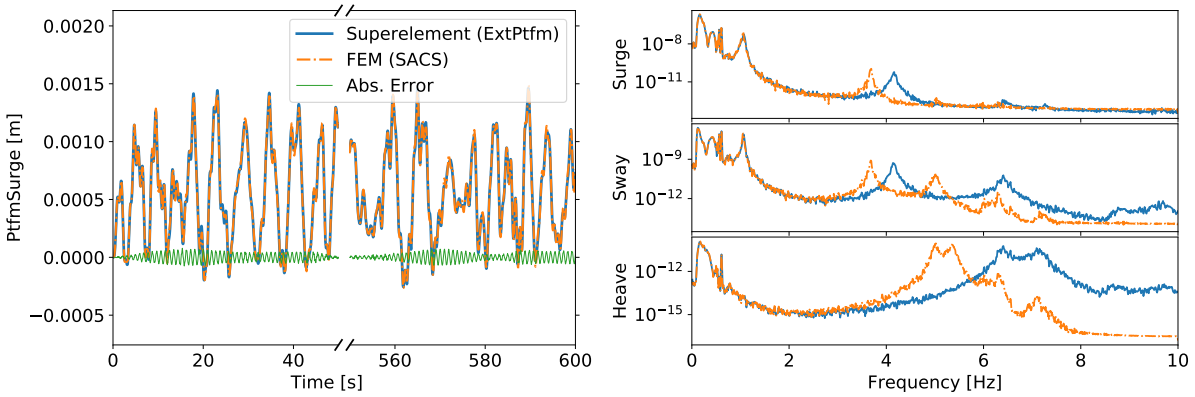

Figure 6: Jacket under hydrodynamic loading. Comparison of platform displacements for FEM and superelement representation of the OC4 jacket subjected to wave loading. (Left:) Time series of surge (Right:) Power spectral density of surge, sway, and heave.

simulation for the full 600 s of the time series response (only 100 s displayed). The mean relative error between the two signals is 2.8%. Some discrepancies exist in the frequency content of the reduced-order representation where a higher frequency is observed around 4 Hz, compared to the FEM spectrum. However, the overall agreement is strong and the superelement correctly represents the structural dynamics excited by the wave loading.

4.4. Jacket and wind turbine under aerohydrodynamic loading

The subsequent validation tests simulate the OC4 jacket supporting the National Renewable Energy Laboratory's 5-MW wind turbine under wind and wave loading. The test cases consist of an aligned wind/wave case under normal operating condition, and a shutdown case. Results from a misaligned simulation were found to be similar to the aligned case and are not included here for conciseness. The wave time series from subsection 4.3 was used together with a turbulence wind field of a 12-m/s mean. All elastic DOF of the turbines were considered. Turbulent wind loads and turbine controls were activated through the *AeroDyn* and *ServoDyn* modules of *OpenFAST*. In each test case, two *OpenFAST* simulations were performed, both with the same

wind turbine models, but one using the superelement and the other using the fully integrated approach with CB reduction (i.e., method 1 and 3 of Figure 2). Both models use 25 CB modes. The superelement formulated in subsection 4.3 was provided to *ExtPtfm* as the basis for the sequentially coupled method, and the OC4 jacket was simulated in *SubDyn* and *HydroDyn* for the fully coupled approach. Results for the normal operating case are given in Figure 7 and the results for the shutdown case are provided in Figure 8.

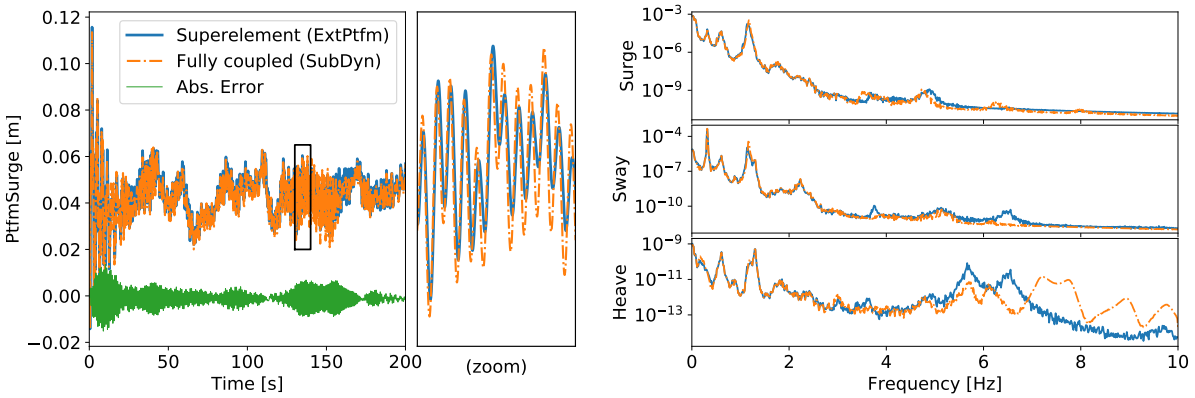

Figure 7: Jacket and wind turbine, aligned case. Platform displacements for the full wind turbine model, as simulated with *OpenFAST* with a superelement representation of the substructure or using the fully coupled *SubDyn* module. (Left:) Time series of surge. (Right:) Power spectral density of surge, sway, and heave.

Results in Figure 7 confirm that the sequentially coupled method satisfactorily represents the fully coupled dynamics of the combined turbine/substructure system. The reduced-order dynamics capture the initial transient response as well as the extended time series. A closer look at the time series reveals that the amplitude of higher frequencies from the fully coupled *OpenFAST* results are not completely matched by the sequentially coupled *ExtPtfm* response; however, the mean relative error between the two time series is 3.7%. The fair agreement of the time series is confirmed by the spectral analysis of Figure 7. The frequency content of the displacements from both simulations correlate well up to a 4 Hz-frequency, above which the agreement deteriorates.

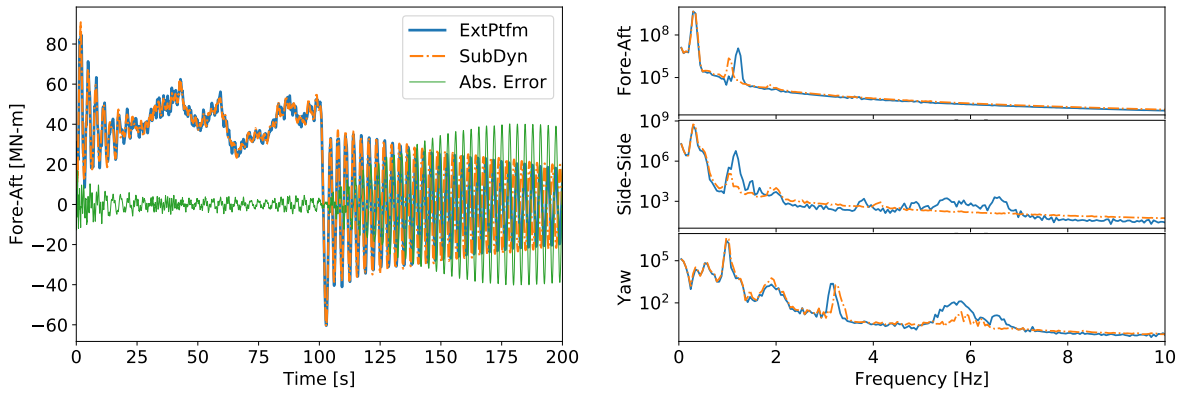

Figure 8: Jacket and wind turbine, shutdown case. Tower base moments obtained using the *ExtPtfm* module or using the fully coupled *SubDyn* module. (Left:) Time series of fore-aft moment. (Right:) Power spectral density of the tower base moments for the period [100-200] s (in units of kN-m)

.

In Figure 8, the tower base moments obtained from *ExtPtfm* and *SubDyn* appear to be consistent, before and after the shutdown event at 100 s. The absolute error is misleadingly large: a drift is progressively building up between the two loadings, which can be attributed to the small differences in the first natural frequency of the models around 0.3 Hz, as was discussed in the interpretation of Figure 5. It is noted that the spectra are shown only for the period following the shutdown, and the symmetry of the jacket implies that similar frequencies are found in the fore-aft and side-side directions. The shutdown case appears to be a more difficult case because it directly reveals differences in the natural frequencies of the models. Yet, both models agree on the loading and displacement (not shown) responses to the shutdown in the few seconds following the event. We conclude that no particular issue is found in using the superelement approach for the shutdown case, despite its potential challenge for the method.

It is important to note that the superelement was not generated by *SubDyn* but by the external FEM software, SACS. We made great efforts to match the FEM representation of *SubDyn* and the sea state used by *HydroDyn* with the ones used by the external software, but many sources of discrepancies may arise in the process, caused by potential differences in: element formulations, discretization, joints modeling, structural damping, wave loads model, rigid connection of the transition piece, and so on. Differences in natural frequencies were, for instance, impacting the analyses of the results given in Figure 8. Despite these potential sources of discrepancies, the results of the superelement and fully coupled simulations showed satisfying agreement. To perform a fair comparison, a superelement generated by the combination of *SubDyn* and *HydroDyn* should be used. Unfortunately, the option to export such a superelement is not available in the current version of these modules.

5. Discussions

The application of the CB reduction technique for sequential simulation of fixed-bottom substructures has been demonstrated in section 4. , additional studies are required to further evaluate the accuracy of the method. Brace-induced vibrations in jackets have been occasionally observed by industrial partners in simulations, using the sequential approach. Whether such vibrations are numerical artifacts of the methods or physical phenomena remains an open question, which is beyond the scope of the current study. A follow-up study should investigate the importance of each factor and further quantify the accuracy and limitation of the method. Such quantification would require statistical analyses on a broader range of test cases, such as the load case suite of the International Electrotechnical Commission design standards. No challenges were identified in section 4, but we still still recommend focusing on events known to be driving loads: wind-wave misalignments, gusts and directional changes, startup and shutdown, and ultimate cases. The study of different jacket designs, and particularly designs that show brace vibrations, if available, would also be highly relevant for the practitioners. The different factors that can affect the accuracy of the method are discussed next.

Mode selection Of key importance for the simulation accuracy is the number of CB modes retained and the choice of these modes. The method is expected to converge to the full model response as the number of modes is increased. Yet, the benefit of the method lies in the possibility to reduce the number of DOF of the model. A common method of mode selection consists of using the modes with the lowest frequencies. In the report from DNV-GL [18], the authors mention this possibility to include a set of high- and low-frequency modes. Once the modes are selected, a modal assurance criteria analysis [19] can help the user determine the accuracy of the reduced-order model and identify the quality of the mode shapes of the reduced-order structure. A comparison of the frequencies between the full FEM model and the reduced model also give insight on the quality of the model and provide an estimate of the cutoff frequency of the reduction. The first frequency of the constrained system is usually a good indicator of

the frequency above which the quality of the model will deteriorate. In general, reduction has the effect of applying a constraint that stiffens the system, resulting in an overestimation of the eigenfrequencies.

Gravity-buoyancy mode As noted by Bredmose et al. [20], the deflection induced by gravity and buoyancy is not considered in the standard CB method since the interface nodes are fixed during the determination of the modes. This omission was shown to lead to decreased performance and possible stationary offsets between the loads obtained from the full and reduced-order models. The method presented in this paper may be extended to include the gravity-buoyancy mode, as described, for instance, by Wang et al. [10]. It is noted that this correction is different from the static improvement method implemented, for example, in *SubDyn*. The static improvement method is important for calculating the internal reaction loads within the substructure but is not relevant for calculating the load transmitted back to the interface. Also, the static improvement method requires the full FEM matrices, which are generally not provided in the superelement exchange process.

Selection of leader DOF For a traditional support structure, the leader DOF are naturally selected as the 6 degrees of freedom at the interface between the substructure and the tower. In the more general context of the CB reduction, some guidelines may be used for the selection of the leader DOF: the DOF without inertia and external load can be condensed without affecting the accuracy; DOF with large mass-over-stiffness ratios are good candidates for leader DOF; and translational DOF also form good candidates, as they usually carry "more information". than rotational DOF.

Nonlinearity The CB method is inherently a linear approach because the system is reduced to a linear set of equations. The absence of nonlinear effects, such as geometrical and inertial nonlinearities or external loads caused by fluid-structure interactions, is a source of error of the sequential approach that cannot be alleviated.

Initialization and transients Structural dynamics tools do not always start at an equilibrium position, and transients are present at the initialization of the simulations (see e.g., Figure 7). The simulation period is typically increased by 50 s to account for this, and the first 50 s of the simulation are then discarded in the postprocessing calculations (e.g., statistics, fatigue, ultimate loads). We recommend keeping the initialization period in the files that are exchanged between both parties so that the target simulation period can be obtained after truncation of the transients. The loads can also be progressively applied during the initialization time to avoid accumulating the transient effects from both tools.

Numerical errors Several sources of numerical errors may be introduced in the process. The numerical resolution of the superelement files being exchanged is important for the precision of the simulation. ASCII file formats with fixed precision are commonly used. Binary files with double precision floats or scaled integers should be preferred to ensure minimum loss of information in the data transfer. This point should be considered both for the time series and the matrices exchanged. Further errors may arise from the temporal discretization used between the two sequential simulation tools. The load time series are often provided at a coarse time resolution (≈ 0.05 s), leading to a cutoff of high frequencies, and linear interpolation schemes used to obtain data at intermediate time steps can result in interpolation errors. Finally, FEM softwares typically use energy-conserving, time-integration schemes such as the Newmark scheme, which are convenient to solve systems with large numbers of DOF. Various numerical schemes with different time steps or substeps may be used by the superelement solver, and such differences may be a potential source of error.

Number of shape functions Tools based on the Rayleigh-Ritz reduction approach, such as *OpenFAST* or *Flex*, rely on a few carefully selected shape functions to represent the dynamics of the tower and the blade. The range of modal frequencies relevant for jacket substructures tends to be broader than for monopiles. The higher frequencies introduced by the substructure may interact with the rest of the structure. To capture this interaction, additional blade and tower shape functions (resulting in higher-frequency content) may be necessary.

Specificities related to *OpenFAST* modeling To increase the frequency content of the model, we suggest using the *BeamDyn* module of *OpenFAST* to represent the blade when accurate blade modeling is required. The *ElastoDyn* module is currently limited to two shape functions for the tower in each direction. Future work should consider increasing this number. The lack of torsional DOF for the tower in *OpenFAST* leads to instability when both the nacelle-yaw and platform-yaw DOF are turned on. We recommend setting the "platform yaw inertia input" to the torsional inertia of the tower to remedy this.

6. Conclusions and future work

The newly implemented module, *ExtPtfm*, is now publicly available and can be used within the open-source wind turbine simulation tool *OpenFAST*. Validation results and potential limitations of the sequentially coupled methodology for load prediction were reported and discussed in the context of recommended industry practices. Guidelines for the usage of the CB technique were provided to ensure the accuracy of the simulation results. Quantitative investigations on the accuracy of the method are yet required. Future work will focus on adding the gravity/buoyancy mode to the model for improved accuracy and adding options for placing the interface node at a different location than the tower bottom. Further, the possibility of exporting superelements from *SubDyn* will be considered to ensure that the superelement and the fully coupled analyses are based on exactly the same structure. The current implementation may be used with floating substructures, either with the superelement including the mooring loads, or by having the mooring loads transferred via the tower-base interface node. Additional support for flexible floating substructures is currently being developed as part of the *SubDyn* and *HydroDyn* modules.

Acknowledgments

This work was authored by the National Renewable Energy Laboratory, operated by Alliance for Sustainable Energy, LLC, for the U.S. Department of Energy (DOE) under Contract No. DE-AC36-08GO28308. Funding provided by the U.S. Department of Energy Office of Energy Efficiency and Renewable Energy Wind Energy Technologies Office. The views expressed in the article do not necessarily represent the views of the DOE or the U.S. Government. The U.S. Government retains and the publisher, by accepting the article for publication, acknowledges that the U.S. Government retains a nonexclusive, paid-up, irrevocable, worldwide license to publish or reproduce the published form of this work, or allow others to do so, for U.S. Government purposes.

References

[1] S. N. Voormeeren, P. L. C. van der Valk, B. P. Nortier, D-P. Molenaar, and D. J. Rixen. Accurate and efficient modeling of complex offshore wind turbine support structures using augmented superelements. *Wind Energy*, 17(7):1035–1054, 2014.

[2] L. Alblas and W. Collier. Implementing an interface between Bladed and Sesam, verification report of Sesam's Bladed interface. Technical report, DNV GL report no. 2016-0866, Rev. 1, 2017.

[3] TC88 WG3. *IEC 61400-3 Wind turbines : Design requirements for offshore wind turbines.* IEC, 2005.

[4] R. Craig and M. Bampton. Coupling of Substructures for Dynamic Analysis. *AIAA Journal*, 6(7):1313–1319, 1968.

[5] R. Guyan. Reduction of stiffness and mass matrices. *AIAA Journal*, 3:380, 1965.
[6] S.N. Voormeeren, P.L.C. van der Valk, and D.J. Rixen. Practical Aspects of Dynamic Substructuring in Wind Turbine Engineering. In *Proceedings of the IMAC-XXVIII 2010, Jacksonville, Florida, USA*, 2010.
[7] R. Damiani, F. Wendt, W. Musial, Z. Finucane, L. Hulliger, S. Chilka, D. Dolan, J. Cushing, D. O'Connell, and S. Falk. Fully vs. sequentially coupled loads analysis of offshore wind turbines. Technical Report 68368, NREL, 2013.
[8] T. Hald and M. Høgedal. Implementation of a finite element foundation module in flex5 using Craig-Bampton substructuring. In *Copenhagen offshore Wind 2005*, 2005.
[9] E. Branlard. Flexible multibody dynamics using joint coordinates and the Rayleigh-Ritz approximation: The general framework behind and beyond Flex. *Wind Energy*, 22(7):877–893, 2019.
[10] S. Wang, T. J. Larsen, and A. M. Hansen. Validation of superelement modelling of complex offshore support structures. In *Proceedings of 12th EAWE PhD Seminar on Wind Energy in Europe*. European Academy of Wind Energy, 2016.
[11] OpenFAST. Open-source wind turbine simulation tool, available at `http://github.com/OpenFAST/OpenFAST/`.
[12] SACS. Offshore structural analysis and design software, produce available at `https://www.bentley.com/en/products/brands/sacs`.
[13] J. Jonkman R. Damiani and G. Hayman. Subdyn user's guide and theory manual. Technical Report NREL/TP-5000-63062, National Renewable Energy Laboratory, 2015.
[14] J. Jonkman. The New Modularization Framework for the FAST Wind Turbine CAE Tool. Technical Report NREL/CP-5000-57228, National Renewable Energy Laboratory, 2013.
[15] M. A. Sprague, J. M. Jonkman, and B. J. Jonkman. FAST Modular Framework for Wind Turbine Simulation: New Algorithms and Numerical Examples. Technical Report NREL/CP-2C00-63203, National Renewable Energy Laboratory, 2015.
[16] W. Popko, F. Vorprahl, A. Zuga, M. Kohlmeier, J. Jonkman, and A. Robertson. Offshore Code Comparison Collaboration Continuation (OC4), Phase I - Results of Coupled Simulation of Offshore Wind Turbine with Jacket Support Structure. In *International Offshore and Polar Engineering Conference*, volume 1, pages 337–346, Rhodes, Greece, 2012. International Society of Offshore and Polar Engineers.
[17] R. Damiani and F. Wendt. Assessment of Sequentially- Versus Fully-Coupled Dynamic Analysis of Offshore Wind Turbines. Technical report, NREL, 2017.
[18] DNV GL. Implementing an interface between Bladed and Sesam - Verification report of Sesam's Bladed interface. Technical Report 2016-0866, Rev. 1, Risø-DTU, 2017.
[19] R. Allemang and D. Brown. A correlation coefficient for modal vector analysis. In *Proceedings of the International Modal Analysis Conference. Society for Experimental Mechanics: Bethel, CT, USA.*, page 110–116, 1982.
[20] H. Bredmose, J. Mariegaard, Bo Terp P., B. Jensen, S. Schløer, T. J. Larsen, T. Kim, and A. M. Hansen. *The Wave Loads project*. DTU Wind Energy, Denmark, 2013.